Applied Catalysis A, General 624 (2021) 118327

Contents lists available at ScienceDirect

Applied Catalysis A, General

journal homepage: www.elsevier.com/locate/apcata

Production of ethyl lactate by activated carbon-supported Sn and Zn oxide catalysts utilizing lignocellulosic side streams

Riikka Kupila [a,b,*], Katja Lappalainen [a,b], Tao Hu [b], Anne Heponiemi [b], Davide Bergna [a,b], Ulla Lassi [a,b]

[a] Unit of Applied Chemistry, Kokkola University Consortium Chydenius, University of Jyväskylä, P.O. Box 567, FIN-67101, Kokkola, Finland
[b] Research Unit of Sustainable Chemistry, University of Oulu, P.O. Box 4300, FIN-90014, Oulu, Finland

ARTICLE INFO

Keywords:
Activated carbon
Heterogeneous catalyst
Metal oxide
Ethyl lactate
Lignocellulosic biomass

ABSTRACT

In this study, activated carbon-supported Sn and Zn oxide catalysts were prepared from hydrolysis lignin and used for the conversion of model solutions of trioses, hexoses, and lignocellulosic biomass hydrolysates to ethyl lactate. Both catalysts, SnO_2@AC and ZnO@AC, were able to produce ethyl lactate in high yields. SnO_2@AC was a more active and selective catalyst in triose (dihydroxyacetone) conversion, providing 99% yield to ethyl lactate. ZnO@AC, by contrast, was more selective in glucose and hydrolysate conversion, with a yield of 60% and 85%, respectively. The ethyl lactate yields were significantly higher than those from the optimized model solution experiments when using ZnO@AC catalyst. These findings indicate that milder acidity of the ZnO@AC catalyst together with Na^+ and SO_4^{2-} in hydrolysate favored ethyl lactate production, preventing byproduct, furan derivatives and acetal, formation. Moreover, the catalysts were able to maintain their catalytic activity in recycling experiments.

1. Introduction

Development of novel heterogeneous catalysts for the conversion of biomass to high-value chemicals and materials is attractive from environmental and industrial perspectives. Growing industrial interest in the production of chemicals from biomass resources, such as lactic acid and its esters, alkyl lactates, has attracted much attention in recent years since they can be considered as one of the most promising building block monomers and green solvents today. Lactic acid can be used as a building block molecule for several downstream chemicals, such as acrylic acid and propylene glycol, with applications in polyesters, carbonates, and urethanes, as well as for poly(lactic acid) plastics for example [1,2]. Alkyl lactate hydrolysis is also one of the methods used to obtain lactic acid [1,3]. Alkyl lactates such as methyl and ethyl lactate can be used as promising bio-based, renewable, non-carcinogenic, and biodegradable green solvents [1,4–6]. These could be used as substitutes for several environment-damaging halogenated and toxic solvents [7–9]. The most prominent alkyl lactate is ethyl lactate, a short chain ester that combines a high boiling point, low vapor pressure, and low surface tension with its renewable origin [1,10,11].

Lactic acid and its lactates can be generated from biomass raw materials through chemical synthesis or fermentation routes [1]. The production through fermentation process is the most common; however, drawbacks of such processes include the need for expensive and energy-inefficient separation and purification steps [11,12]. The development of an alternative, sustainable, heterogeneous catalytic method for producing lactic acid and lactates from renewable sources would be of great relevance. The main challenges in the production of lactic acid with heterogeneous catalysts are relatively low yields and the formation of undesired byproducts deactivating the catalyst when using water as a solvent [11–14]. When water is replaced with ethanol, ethyl lactate can be produced through heterogeneous catalysis directly from biomass precursors. The production of ethyl lactate with heterogeneous catalysts has its advantages: long life time of the catalyst, side reactions can be eliminated or are less significant, ease of separation from the reaction mixture by distillation, and working in a recyclable alcoholic media [1,11,15]. The heterogeneous catalysts studied in the conversion of biomass-based molecules, such as trioses, pentoses, hexoses, and native biomasses, to lactates have mainly been Sn-based catalysts [2,16,17]. In many studies, hierarchical zeolites and supported catalysts have

* Corresponding author at: Unit of Applied Chemistry, Kokkola University Consortium Chydenius, University of Jyväskylä, P.O. Box 567, FIN-67101, Kokkola, Finland.
E-mail address: riikka.kupila@oulu.fi (R. Kupila).

https://doi.org/10.1016/j.apcata.2021.118327
Received 6 April 2021; Received in revised form 15 August 2021; Accepted 16 August 2021
Available online 18 August 2021

been used. The proposed reaction path of converting biomass and biomass-based molecules is believed to proceed through glucose isomerization to fructose and further through multiple reactions to trioses, such as dihydroxyacetone (DHA), glyceraldehyde, and pyruvaldehyde, and the eventual esterification of lactic acid with alcohol to its corresponding alkyl lactate (Scheme 1)[17,14]. The yields of lactate from hexoses have generally been lower than those obtained from trioses [15]. Sn/Al_2O_3 catalysts converted trioses (DHA) in EtOH to ethyl lactate up to 68% yield [18]. Sn-Beta-H catalysts were used in glucose conversion to ethyl lactate with a yield of 29–41% at 160 °C under N_2 in 10-20 h [19–21]. Conversion of fructose to ethyl lactate over oxide catalysts—SnO_2, $10SnO_2/Al_2O_3$ and $10SnO_2$-$5ZnO/Al_2O_3$—was studied by Prudius et al., who obtained yields of 2%, 32%, and 56%, respectively (160 °C, 60 rpm, 3 h) [22]. Direct conversion of rice straw to lactate with $SnCl_2/SnCl_4$, $SnCl_2$/ZSM-5, and $SnCl_2/\gamma$-Al_2O_3 catalysts yielded up to 21.8%, 20.0%, and 17.1% of ethyl lactate, respectively, in 4 h at 220 °C in sub-critical ethanol [23].

The main aim of this study was to produce activated carbon-based heterogeneous catalysts for the production of ethyl lactate as efficiently and selectively as possible from lignocellulosic precursor materials. Activated carbon supports are known to have large surface areas, high pore volumes, surface functional groups induced acid base properties, and relatively high mechanical strength, due to which they have already been applied in specific biomass valorization processes [25]. As a precursor for activated carbon catalyst support, hydrolysis lignin, a waste fraction from biomass hydrolysis, is used and modified with nitric acid treatment to contain oxygen functional groups. Sn or Zn oxides on activated carbon support were prepared by impregnation method. The prepared catalysts were characterized by multiple analysis methods, and the activity of these materials was studied for conversion of model solutions of dihydroxyacetone, fructose, and glucose in a batch reactor in ethanol under nitrogen atmosphere. Besides the model solutions, the real biomass solutions obtained from lignocellulosic biomass hydrolysis, fiber sludge and spruce, were tested in catalytic conversion to ethyl lactate. Stability of the catalysts in recycling experiments was also studied. To the best of our knowledge, activated carbon-supported metal oxide catalysts have not been used in the conversion of biomass-based molecules to ethyl lactate.

2. Materials and methods

2.1. Chemicals

Hydrolysis lignin from the biomass hydrolysis process was obtained from Sekab, Sweden. Fiber sludge was obtained from Domsjö Fabriker AB, Sweden, and hydrolysis was performed by Processum (Sweden) through enzymatic hydrolysis with commercial enzymes followed by filtration to remove solids.

Spruce hydrolysate obtained from Sekab AB, Sweden, was prepared from unbarked Norway spruce by pretreatment with steam and sulfur dioxide. After pretreatment, enzymatic hydrolysis was performed with commercial enzymes followed by separation of solids and adjustment of pH with NaOH [26].

The following catalyst preparation materials were used: anhydrous $SnCl_2 \cdot 2H_2O$ (99%) from Merck, $Zn(NO_3)_2 \cdot 6H_2O$ (99%) from Alfa Aesar, and HNO_3 (65%) from Merck. Anhydrous glucose (99%) from Alfa Aesar, fructose (99%) from Acros Organics, ethanol absolute (99.97%) from VWR, ethyl L-lactate (99%) from Alfa Aesar, ethyl levulinate (98%) Alfa Aesar, dihydroxyacetone (98%) Merck, 5-(hydroxymethyl)furfural (HMF) (98%) from Acros Organics, anhydrous lactic acid (98%) from Alfa Aesar, and levulinic acid (98%) from Acros Organics were used as reagents and/or standard materials.

2.2. Catalyst preparation

The activated carbon support was prepared from hydrolysis lignin by physical activation using steam. Preparation process was proceed similarly as in our previous study [27]. Carbonization, followed by physical activation of the biomass with steam, was performed in a rotating quartz tube in a tube furnace using a heating ramp of 10 °C min^{-1} to a temperature of 800 °C. At the 800 °C, steam was added by feeding water at a flow rate of 0.5 mL min^{-1} into the reactor for 2 h. During the thermal heating process, the reactor was flushed continuously with inert N_2 gas. The resulting activated carbon support was sieved to a fraction size of 0.1–0.42 mm. The treatment of the support with 3 mol L^{-1} HNO_3 was selected for use in this study to remove the residual metal content originating from biomass and to modify the surface. Based on our previous study, the production of lactic acid with activated carbon catalysts, the nitric acid treated (oxidized) carbon supports, performed better than untreated ones [27]. The treatment was carried out in a round-bottom flask with a ratio of 10:1 mass ratio of acid:support, mixed, and heated for 4 h at 85 °C. After the acid treatment, the supports were filtrated and washed with hot distilled water until a constant pH was obtained and dried in the oven at 105 °C.

Impregnation was performed by the incipient wetness method, and the pore volumes of the support materials were measured by the N_2-physisorption method to calculate the volume of the impregnation solution. The amount of metal salts ($SnCl_2 \cdot 2H_2O$ and $Zn(NO_3)_2 \cdot 6H_2O$) added by impregnation on the support was calculated by assuming the targeted concentration of metal (Sn or Zn) in the catalyst was 10 wt.% of the total catalyst mass. Zn salt was added in distilled water to dissolve the precursor salt. To dissolve Sn salt, a drop of concentrated HCl was added in distilled water. The impregnation solution was mixed with the support, matured for 4–5 h at room temperature, and finally dried in an oven at 105 °C for 16 h. The catalysts were thermally treated in a quartz tube in a tube furnace under a nitrogen atmosphere using a constant flush of N_2 (at a flow rate of 10 mL min^{-1}). The thermal treatment was carried out at 350 °C, using a 5 °C min^{-1} ramp and a 3 -h holding time at the target temperature.

2.3. Catalyst characterization

Specific surface areas (SAs) and pore size distributions were determined from the physisorption adsorption isotherms using nitrogen as the adsorbate. Determinations were performed with a Micromeritics ASAP 2020 instrument (Micromeritics Instrument, Norcross, GA, USA). Portions of each sample (0.2 g) were degassed at a low pressure (0.27 kPa) and a temperature of 140 °C for 3 h to remove the adsorbed gas.

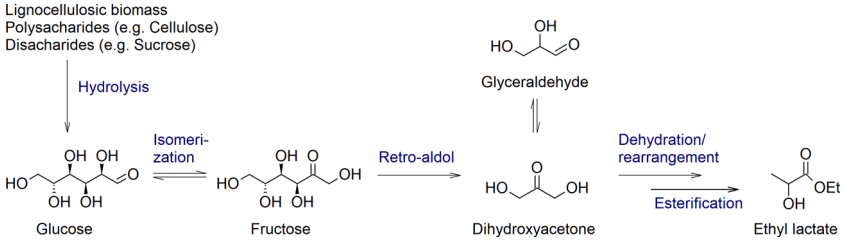

Scheme 1. Reaction scheme for the conversion of biomass-based molecules into alkyl lactates in EtOH [17,24].

Adsorption isotherms were obtained by immersing the sample tubes in liquid N_2 (−196 °C) to achieve constant temperature conditions. Gaseous nitrogen was added to the samples in small doses, and the resulting isotherms were obtained. SAs were calculated from the adsorption isotherms according to the Brunauer–Emmett–Teller (BET) method. The precentral distribution of pore volumes (vol.%) was calculated from the individual volumes of micropores (pore diameter < 2 nm), mesopores (pore diameter 2–50 nm), and macropores (pore diameter > 50 nm) using the density functional theory (DFT) model.

The morphology of the catalyst particles was studied using a JEOL JEM-2200FS energy-filtered transmission electron microscope (EFTEM) equipped for scanning transmission electron microscopy (STEM). The STEM model is used for images, energy-dispersive X-ray spectroscopy (EDS) analysis and quantitative mapping of the catalyst. The catalyst samples were dispersed in pure ethanol and pretreated in an ultrasonic bath for several minutes to create a microemulsion. A small drop of the microemulsion was deposited on a copper grid pre-coated with carbon (Lacey/Carbon 200 mesh copper) and evaporated in air at room temperature. The accelerating voltage in the measurements was 200 kV, while the resolution of the STEM image was 0.2 nm. The metal particle sizes were estimated visually from the high-resolution STEM images of each sample.

The metal contents of the supports and catalysts were measured by ICP-OES using a Perkin Elmer Optima 5300 DV instrument. Samples weighing 0.1–0.2 g were first digested with 9 mL of HNO_3 at 200 °C for 10 min in a microwave oven (MARS, CEM Corporation). Then, 3 mL of HCl was added, and the mixture was digested at 200 °C for 10 min. Finally, 1 mL of HF was added, and the mixture was again digested at 200 °C for 10 min. Excess HF was neutralized with H_3BO_3 by heating at 170 °C for 10 min. Afterwards, the solution was diluted to 50 mL with water, and the elements were analyzed using the ICP-OES method.

X-ray diffractograms were recorded with PANalytical X'Pert Pro X-ray diffraction (XRD) equipment using monochromatic CuKα1 radiation (λ = 1.5406 Å) at 45 kV and 40 mA. Diffractograms were collected in the 2θ range of 5°–80 ° at 0.017 ° intervals, with a scan step time of 110 s. The crystalline phases and structures were analyzed using the HighScore Plus program.

X-ray photoelectron spectroscopy analyses were performed using the Thermo Fisher Scientific ESCALAB 250Xi XPS System. The catalyst samples were placed on an indium film with a pass energy of 20 eV and a spot size of 900 μm; the accuracy of the reported binding energies (BEs) was ±0.3 eV. Sn, Zn, O, C, Cl, and N elemental data were collected for all samples. The measured data were analyzed with Avantage V5 software. The monochromatic AlKα radiation (1486.7 eV) was operated at 20 mA and 15 kV. Charge compensation was used to determine the presented spectra, and the calibration of the BEs was performed by applying the C1s line at 284.8 eV as a reference. The approximate detection depth of the analysis was < 10 nm.

Acidity of the samples was monitored with ammonia temperature-programmed desorption (TPD) analysis using a Micromeritics AutoChem II 2920. Pretreatment of the sample (50 mg) was done at 350 °C for 30 min under a helium flow (50 cm^3 min^{-1}) and then cooled to 100 °C. Subsequently, 5% ammonia in the helium flow (50 cm^3 min^{-1}) was absorbed on the sample at 100 °C for 1 h, after which the dry helium flow for 30 min was used to remove the excess ammonia on the catalyst surface. Finally, NH_3-TPD was carried out from 100 °C to 600 °C at the ramp of 10 °C min^{-1} in the dry helium flow.

The total acidity and basicity of the surfaces of AC and catalysts were characterized by the acid-base back-titration method [28,29]. The samples (0.1 g) were weighed and separately mixed with 50 mL of 0.01 mol L^{-1} solutions of HCl or NaOH, and shaken for 72 h in sealed vials at room temperature. The solutions were filtered with a 0.45 μm membrane filter. Acidic groups were determined by the back-titration method—taking 10 mL of filtrate of NaOH, mixing with 20 mL of 0.01 mol L^{-1} HCl and finally back-titrating with 0.01 mol L^{-1} NaOH using potentiometric titration. The total acidic group concentration was calculated assuming that NaOH neutralizes the acidic sites on the surface. Basic sites were calculated vice versa by back-titration with 0.01 mol L^{-1} HCl; the total number of basic groups was calculated with the assumption that HCl neutralizes the basic groups on the surface.

Ion chromatography (761 Compact IC, Metrohm) was used to determine the anion contents (SO_4^{2-}, PO_4^{3-}, Cl-, NO_3- and F-) of the biomass hydrolysates. The liquid samples were analyzed with Metrosep A Supp 5 column (100/4.0 6.1006.510) with pre-column Metrosep A Supp 5 guard/4.0 using 0.5 mM $NaHCO_3$ + 1.5 mM $NaCO_3$ as a mobile phase with a flow rate of 1.0 mL min^{-1}.

Capillary electrophoresis was used to determine the contents of the carbohydrates galactose, glucose, sucrose, mannose, arabinose, xylose, and ribose from the biomass hydrolysates with Hewlett Packard HP^{3D}CE. Monitoring of carbohydrates was carried out using direct UV detection at a wavelength of 270 nm with a bandwidth of 10 nm. Silica capillaries (CE4-ORG) of 50 μm I.D. and length 56 cm were employed in the experiments with buffer 160 mM NaOH + 36 mM Na_2HPO_4, pH 12.6.

2.4. Catalyst performance tests

For catalyst testing, HEL's manual DigiCAT pressure reactor with the hotplate and stirrer system and three parallel Mini-Range stainless steel reactors (50 mL), each with individual manometers for pressure control, was used. In a typical reaction, the catalyst (0.1 g) was added to the reactor with 0.2 g (2.2 mmol) of DHA or 0.1 g of fructose or glucose (0.55 mmol) in 20 mL of ethanol. When hydrolysates were used, the amount of substrate added to the reaction was calculated to be equal to the glucose molar amount (0.55 mmol) in 20 mL of EtOH. The reaction mixture was mixed continuously at 600 rpm and the reactor was purged with nitrogen five times to remove the inside air. The heating was started after purging with nitrogen. When a reaction temperature of 160 °C was reached (in about 25 min), the reactor pressure was about 10 bar. The temperature was maintained constant through the heating of the external aluminum block in which the parallel reactors and external temperature probe were placed. Samples were collected during the reaction. After the required reaction time, samples (about 1 mL) were collected from the reactor through the outlet vent and filtrated with a 0.45 μm (polyethersulfone) membrane filter for further product analysis. Two tests were run in parallel, and the error was presented as a percentage of the average standard deviation of the two parallel tests. Recycling of the catalyst was performed after filtering out the catalyst from the reaction solution and washing it with ethanol. The catalyst was then used under the same reaction conditions as in the previous cycle. Due to collection loss, the weight of the catalyst was slightly lower than the initial weight after recycling; the corresponding glucose loading was reduced to keep the weight ratio of the catalyst to glucose constant.

Compounds from product mixture were identified (qualitative analysis) using an Agilent 8890 GC System equipped with a mass detector (MS) and an Agilent HP5-MS Ultra Inert GC column (30 m x 0.25 mm x 0.25 mm). The oven temperature was programmed at 70 °C for 1 min, then increased to 280 °C at 10 °C min^{-1} and kept there for 5 min. The injection volume was 1 mL and He flow 1 mL min^{-1}. Mass spectra were collected with an electron impact ionization of 70 eV. The full-scan acquisition was performed with the mass detection range set at m/z 35–500. Data acquisition and analysis were executed using 5977B GC/MDS (Agilent Technologies).

The product analysis (quantitative analysis) was performed with a Shimadzu high-performance liquid chromatograph (HPLC) equipped with a Shodex RI and UV detector. The quantification was based on external calibration using standard solutions of glucose, fructose, dihydroxyacetone, ethyl lactate, lactic acid, levulinic acid, ethyl levulinate and HMF, furfural, formic acid, acetic acid, and ethyl formate. The liquid samples were analyzed with a Shodex SUGAR SH1821 column (8.0 mm ID × 300 mm) with pre-column SUGAR SH-G using 5 mM H_2SO_4 as a mobile phase with a flow rate of 1.0 mL min^{-1} and a column temperature

of 40 °C. Conversion, yield, and selectivity were calculated from the results of the quantification by HPLC using the following equations:

$$\text{Conversion } (\%) = \frac{C_{substrate\ initial} - C_{substrate\ at\ end\ of\ reaction}}{C_{substrate\ initial}} \quad (1)$$

$$\text{Yield } (\%) = \frac{C_{measured\ ELa\ in\ the\ sample}}{C_{theoretical\ max.\ of\ ELa\ in\ the\ sample}} \quad (2)$$

$$\text{Selectivity } (\%) = \frac{Yield}{Conversion} \quad (3)$$

The theoretical maximum of ethyl lactate in the sample (Eq. 2) was calculated by assuming that 1 mol of ethyl lactate was obtained from 1 mol of triose (DHA) as a substrate and 2 mol of ethyl lactate was obtained from 1 mol of hexose (glucose or fructose) as a substrate. When biomass hydrolysate was used as a substrate, the conversion and ethyl lactate yield were calculated from the initial glucose content.

3. Results and discussion

3.1. Catalyst characterization

Properties of the prepared and HNO_3 treated activated carbon and catalysts were studied through multiple characterization techniques. The BET SAs, average pore diameters, and DFT pore volumes and pore distributions of the AC support and catalysts were measured by N_2-physisorption analysis, and the results are listed in Table 1. The results of the physisorption measurements showed that nitric acid-treated AC had a high BET surface area containing a micro-mesoporous pore distribution 1:1 ratio. When metal salts were impregnated on AC, catalysts SnO_2@AC and ZnO@AC had rather similar high BET surface areas and pore volumes, which decreased from the original AC during the impregnation process, indicating the metal addition on the surface and mesopores. The targeted metal content of Sn and Zn in each of the catalysts was 10 wt.%. The measured metal content by ICP-OES analysis was 7.4 wt.% of Sn in SnO_2@AC and 9.9 wt.% in ZnO@AC catalyst. Tin is rather difficult to evaluate with ICP-OES analysis, and this is probably why the Sn content showed lower amount than expected. Further, the metal contents and phases were analyzed with STEM combined with quantitative mapping and XPS analysis.

XRD analysis was performed to verify the metal phases of the catalysts. The diffraction patterns are presented in Fig. 1a. For AC support and catalysts, broad peaks at 2θ 23.8 ° and 44.2 ° were detected, representing carbon. From the catalysts, oxidized metal phases were detected according to the XRD patterns. For ZnO@AC, peaks at 2θ 31.7 °, 34.3 °, 36.1 °, 47.4 °, 56.5 °, 62.7 °, 67.8 °, and 68.9 °, representing zinc oxide (ZnO) (JCPDS file No. 04-003-2106) were detected. For SnO_2@AC, at 2θ 26.3 °, 33.5 °, 51.7 °, and 64.2 ° representing tin(IV) oxide (SnO_2) (JCPDS file No. 00-001-0657) was detected. The degree of crystallinity observed from the XRD analysis was different for ZnO@AC and SnO_2@AC catalysts. For Sn, broad peaks were detected, most likely because of the small tin particle size, which were also observed in the STEM images.

Based on the STEM images (Fig. S1 and Fig. S2 in Supplementary material), tin particle size on the SnO_2@AC was smaller (ca. 10 nm) and more evenly distributed on the surface compared to zinc particles on ZnO@AC, which, by contrast, was on the surface as needle-shaped and slightly more aggregated particles. Quantitative mapping of the SnO_2@AC (Fig. S1) showed that catalyst contained 84.0 wt.% of carbon, 6.2 wt.% of oxygen, 8.1 wt.% of tin, and a small amount of chlorine (1.7 wt.%) as a leftover from the preparation process of catalyst was also detected on the surface of the catalyst. Mapping of the ZnO@AC (Fig. S2) presented 84.0 wt.% of carbon, 7.2 wt.% of oxygen, 7.1 wt.% of zinc, and a small amount of nitrogen 1.6 wt.% on the surface of the catalyst. Oxygen was detected all over the carbon; however, it was more concentrated on the metal sites, indicating oxidized metal particles on both catalysts. Observations from the STEM images and quantitative mapping were indicating small Sn particles and a higher amount of Sn on AC detected than it was with ICP-OES analysis.

XPS analysis of the AC and catalysts (Fig. 1 b, Table S1 in supplementary material) revealed main peaks in all samples located at around 284.8 and 531.2 eV assigned to the C1s and O1s spectra, respectively. The peaks from the high-resolution XPS C1s spectra indicated that most of the carbon was present as graphitic conjugated carbon (at 284.8 eV) and non-conjugated carbon (at ~285 eV). Carbon-oxygen type functionalities were also present at 286.6 eV (from phenolic, alcoholic, or etheric functional groups) and at 288.8 eV (from carboxylic, anhydride, ester, or lactone groups) [30,31]. The modification with nitric acid created oxygen containing surface groups, which could be seen from the O1s scan at 532.3 eV (Table S1), and can be identified from oxygen functionalities such as lactone, ester, carboxylic or anhydride, and oxygen atoms from phenol or ether groups on AC. The HNO_3 modification effect to the AC is reported in detail in our previous study [27]. Further, some nitrogen functionalities on AC could be detected from N2p spectra. Fig. 1c shows spectra of XPS Sn 3d, with two peaks at 487.7 and 496.1 eV corresponding to binding energies of Sn $3d_{5/2}$ and Sn $3d_{3/2}$, respectively, assigned to Sn^{4+} [32]. O1s of the SnO_2@AC catalyst showed (Table S1 and Fig.S3a in supplementary material) that the core level peak could be resolved into three components centered at 530.6 eV, 531.5 eV and 532.5 eV, indicating, most likely, the presence of oxidized tin and oxidized carbon functionalities in catalyst as O-Sn^{4+}, Sn-O-C and/or C = O and C-O, respectively [33][32]. Tin content on the surface of SnO_2@AC according to XPS Sn $3d_{5/2}$ at 487.7 eV was 9.5%. As shown in Fig. 1 d, the Zn 2p core level of ZnO@AC had two fitting peaks located at 1045.7 eV and 1022.6 eV corresponding to Zn $2p_{1/2}$ and Zn $2p_{3/2}$, respectively, indicating the chemical valence of Zn^{2+}[34]. From XPS O1s spectra of ZnO@AC (Table S1 and Fig. S3 b in supplementary material), the peak interpretation revealed, most likely, the presence of oxidized zinc and carbon functionalities as Zn-O at 529.7 eV, Zn-O-C, Zn-OH and/or C = O at 531.4 eV and C-O bonding at 533.2 eV [34,35]. Zinc content on the surface of ZnO@AC according to XPS $Zn2p_{3/2}$ at 1022.6 eV was 7.7%. XPS analysis was in agreement with XRD and STEM analyses.

The acidic sites on the carbon and catalyst surfaces were studied by temperature-programmed desorption of ammonia. The acidic and basic sites were studied by acid-base back-titration. Acid sites on the carbon are considered, for example, carboxyl groups, lactones, and phenol and lactol groups. Basic sites, for example, are chromene, pyrone, or heteroatom-derived groups such as N, P, and S in amine or pyridine groups [36]. Inorganic groups on the surface, such as metal oxides and hydroxides, can affect both acidity and basicity [36]. Metal oxides, such as zinc and tin, are known as amphoteric oxides that can act as a base or an acid. NH_3-TPD is used to get information about acid sites on the surface. The NH_3-TPD profiles (Fig. S4) of support and catalysts revealed three main desorption peaks, detected by a thermal-conductivity detector (TCD), with peak maximum in the range of 180 °C, 400 °C, and 550 °C and can be attributed to NH_3 chemisorbed on weak, medium, and strong acid sites, respectively. Peaks detected from the desorption profiles of AC mainly indicated the presence of medium acid groups. The addition of metal oxides on the support led to an increase of weak acid

Table 1
The N_2-physisorption of the AC and SnO_2@AC and ZnO@AC catalysts.

Sample	Surface area[a] [m^2 g^{-1}]	Pore diameter[a] [nm]	Pore volume[b] [cm^3 g^{-1}]	Micro-pores[b][cm^3 g^{-1}]	Meso-pores[b] [cm^3 g^{-1}]
AC	550	2.7	0.32	0.16	0.16
SnO_2@AC	460	2.0	0.19	0.15	0.04
ZnO@AC	490	2.0	0.23	0.15	0.08

[a] Determined by BET method N_2-physisorption analysis.
[b] DFT model N_2-physisorption analysis.

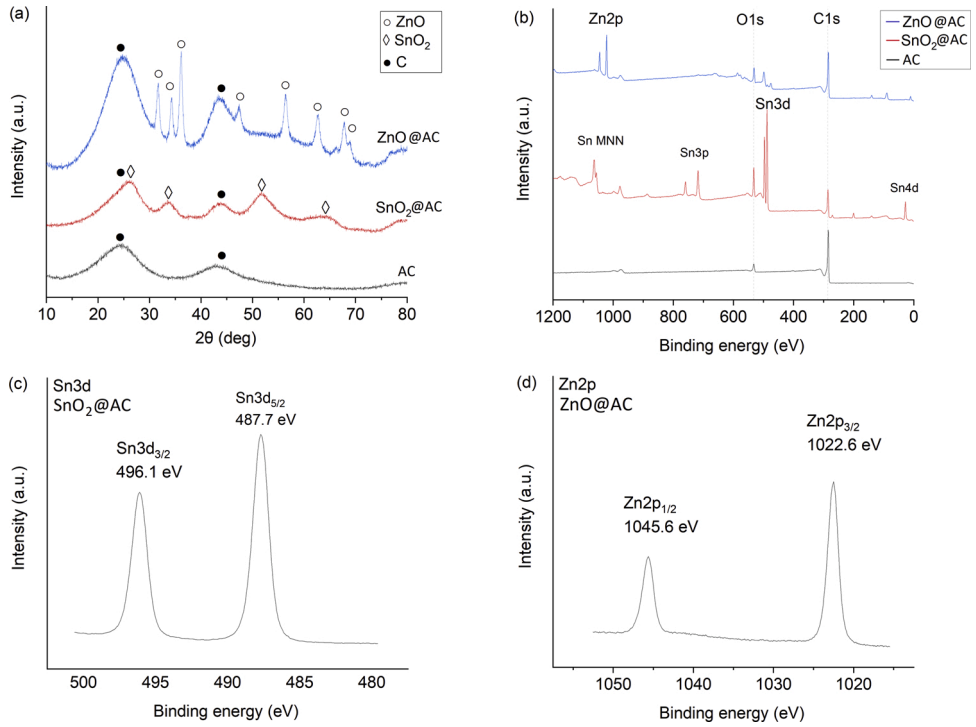

Fig. 1. XRD patterns of the AC and catalysts (a), XPS survey of the AC and catalysts (b), Sn3d of the Sn catalyst (c), and Zn2p of Zn catalyst (d).

sites detected at peak at 180 °C for both catalysts and was higher in ZnO@AC than in SnO_2@AC. In ZnO@AC, weak and medium acid groups were detected. The desorption peak at around 550 °C for the SnO_2@AC catalyst was higher and at higher temperature than those of the support and ZnO@AC. This indicates that Sn species were responsible for generating new and stronger acid sites. It must be noted that, from TPD profiles, it is not possible to discriminate between Brønsted and Lewis acidity. However, it could be assumed that the peak around 400 °C from NH_3-desorption profile of AC could be from the carbon structure containing functional Brønsted acid sites in the medium strength and were also present in the catalysts. The acid-base back-titration method was applied to obtain information about the total acid sites on the surfaces (Table 2). The titration revealed a higher acidic site concentration for the SnO_2@AC catalyst (1.37 mmol g^{-1}) compared to the ZnO@AC catalyst (0.73 mmol g^{-1}) or the support (0.84 mmol g^{-1}) and the amount of acidic sites was almost double in tin catalyst. The total basic group concentration of the samples investigated by the acid-base back-titration method (Table 2) revealed that basic sites could be detected only on the surface of the ZnO@AC catalyst (0.90 mmol g^{-1}) and no basic sites were detected in the AC support or SnO_2@AC. In summary, the measurements indicated that SnO_2@AC was more acidic, containing stronger and higher amounts of acidic sites on the surface than ZnO@AC, which, by contrast, showed both milder acidity and mild basicity of the surface.

3.2. Conversion studies

Catalytic studies with SnO_2@AC and ZnO@AC for the conversion to ethyl lactate were performed from DHA, fructose, and glucose as model solutions and from the real biomass solutions obtained from lignocellulosic biomass hydrolysis, fiber sludge, and spruce.

Table 2
Acidity and basicity of the AC and catalysts.

Sample	Acidic sites [mmol g^{-1}]	Basic sites [mmol g^{-1}]
AC	0.84	0.00
SnO_2@AC	1.37	0.00
ZnO@AC	0.73	0.90

3.2.1. Triose conversion

The conversion of dihydroxyacetone (DHA) was performed by using 0.1 g of the catalyst SnO_2@AC or ZnO@AC and 0.2 g of DHA in 20 mL of EtOH under a nitrogen atmosphere at 160 °C with 600 rpm mixing. The pressure of the reaction solution at 160 °C was about 10 bar in the reactor system. The results of the conversion reactions are presented in the Table 3. Complete conversion of DHA was achieved with the SnO_2@AC catalyst in one hour, and the selectivity and yield to ethyl lactate was >99% after 15 min when the conversion of DHA was already 100%. DHA conversion with ZnO@AC was 92% after 4 h with a yield of 52% ethyl lactate, and the reaction was much slower compared to the SnO_2@AC catalyst. In other studies, triose (DHA) conversion to lactate with high yields (>90%) has been achieved using Sn-beta zeolites [3,17,37,38]. In our study, complete conversion of DHA to ethyl lactate (>99%) was achieved with Sn catalyst within 1 h, however, it must be noticed that reaction conditions i.e. temperature in this study was higher. The combination of Lewis acid together with Brønsted acid sites has been said to improve the activity and selectivity in the conversion

Table 3
Production of ethyl lactate from dihydroxyacetone (DHA), fructose, and glucose with SnO_2@AC and ZnO@AC at 160 °C using 0.1 g catalyst and 0.2 g DHA or 0.1 g glucose/fructose in 20 mL of EtOH.

Feedstock	Catalyst	Time [h]	Conversion [%]	Yield [%]	Selectivity [%]
DHA	AC	1	79	5	6
	SnO_2@AC	1	99	99	99
	ZnO@AC	1	72	15	21
		6	99	52	53
Fructose	SnO_2@AC	6	99	55	54
	ZnO@AC	6	91	54	60
Glucose	AC	6	78	4	5
	SnO_2@AC	6	99	45	45
		24	99	31	31
	ZnO@AC	6	94	37	39
		24	99	48	48

reactions of trioses to ethyl lactate. In a study with mesoporous Sn-MCM-41, a catalyst containing both Lewis and Brønsted acid sites yielded up to 98% ethyl lactate from the conversion of 0.18 g DHA in 6 h (0.2 g cat., 5 mL EtOH at 90 °C) [3]. De Clippel et al. studied Sn-MCM-41 crafted with a carbon network and concluded that the addition of weak Brønsted acid sites due to the oxygen-containing functional groups accelerated the conversion of trioses to lactate; however, they proposed that strong Brønsted acidity increased the acetal formation [17]. In our AC catalysts, the Brønsted acidity arising from the surface acidic oxygen groups or from partially hydroxylated surface oxides seemed to be present, since, for both catalysts, some acetaldehyde diethyl acetal seemed to be produced according to the GC-MS studies (Fig.S5.). Acetaldehyde diethyl acetal is formed from ethanol and acetaldehyde under the presence of a catalyst in acid medium [39,40]. It is possible that ethanol undergoes a dehydrogenation reaction, for example, to form acetaldehyde [41,42]. Carrasco-Marín et al. found that dehydrogenation and dehydration of ethanol to form acetaldehyde can took place on the activated carbon surfaces, especially on oxidized ones [43]. Acetaldehyde in the process, on the other hand, can be formed from pyruvaldehyde converted into formic acid and acetaldehyde or from isomerization of glyceraldehyde into lactic acid followed by decarbonylation to acetaldehyde [44,45]. Besides the acetaldehyde diethyl acetal, other byproducts were formed in the reaction with the ZnO@AC catalyst (see Fig. S5). However, these reactions are not usually detected from the triose conversion with other catalyst materials [3,46], indicating that activated carbon surface participated to the dehydrogenation and dehydration of ethanol.

The ethyl lactate production from DHA with oxidized AC alone was tested in EtOH at 160 °C using 0.1 g of AC and 0.2 g of DHA, and the yield was only 8% after 6 h. This indicated that Brønsted acid sites on the carbon alone were not selective to ethyl lactate production from DHA. With SnO_2@AC, the higher acidity arising from Lewis acid sites, metal oxides, together with Brønsted acid sites, was most likely responsible for the high yield of ethyl lactate from DHA with SnO_2@AC catalyst. However, ZnO@AC with weaker acidic sites did not achieve as good a performance as the SnO_2@AC catalyst in the conversion of DHA to ethyl lactate.

3.2.2. *Hexose conversion*

Conversion of fructose with SnO_2@AC to ethyl lactate was also rather fast. About 99% of the conversion was achieved after 15 min (Table 3). After 15 min, a 42% yield was achieved, which continued to increase to 55% after 4 h and was stable at 6 h (Fig.2). When the ZnO@AC catalyst was used, the conversion reaction of fructose was much slower, and after 15 min, the conversion was 27% and the yield was 15%. The yield increased when the reaction was continued and was 54% after 6 h. The selectivity to ethyl lactate was similar for ZnO@AC and SnO_2@AC after 6 h. The main product, ethyl lactate, was verified from the reaction mixture with GC-MS (Fig. S6. supplementary material). The byproducts from the reaction mixture were verified with GC-MS as well; however, the yields were not quantified. As a byproduct, acetaldehyde diethyl acetal was detected from the reaction solution and was the main byproduct for ZnO@AC catalyst. By contrast, with SnO_2@AC, the product distribution was broader and more byproducts were detected from the reaction solution mixture, such as acetals and furan derivatives (HMF, 5-methylfurfural and ethyl levulinate) (Fig.S6).

The ethyl lactate production from glucose with oxidized AC was tested in EtOH at 160 °C using 0.1 g of AC and 0.1 g of glucose, and the yield was only 4% after 6 h (Fig. 3). This demonstrated that functional sites on carbon alone were not selective to ethyl lactate production. When metal oxides were added to the surface, with SnO_2@AC, the maximum yield of ethyl lactate was 45% after 6 h (Fig. 3). As expected, the yield was lower than the ones obtained from DHA or fructose, and the reaction took longer. This demonstrates that the conversion of glucose to ethyl lactate is limited by the glucose to fructose isomerization step as well as the retro-aldol reaction, which are both catalyzed by Lewis acid. When compared to the SnO_2@AC catalyst, the activity of ZnO@AC was lower than the ethyl lactate yield obtained from glucose and was 37% in 6 h. When the reaction was continued overnight for 24 h, the yield was increased to 48% with ZnO@AC, which was the same as the maximum yield with SnO_2@AC catalyst in 6 h. By contrast, the yield of ethyl lactate decreased with SnO_2@AC when the reaction was continued to 24 h. The GC-MS analysis of the reaction solutions revealed that the product distribution was much wider for SnO_2@AC than for ZnO@AC catalyst (Fig. S7, in Supplementary material), as was observed earlier in the fructose conversion. Acetaldehyde diethyl acetal as a byproduct was identified from the reaction mixture for both catalysts noted earlier. It has also been proposed that glucose can degrade to glycoladehyde and aldotethrose and further to acetal [23]. Interestingly, the selectivity and product distribution for ZnO@AC was more appreciable from hexose than from triose DHA in contrast to SnO_2@AC. With ZnO@AC, the byproduct from the fructose and glucose conversion was mainly acetaldehyde diethyl acetal, compared to SnO_2@AC, which ended up with much wider product distribution. The furan derivatives, such as HMF, ethyl levulinate and 5-methylfurfural, were detected from the product mixture obtained with SnO_2@AC catalyst but were absent when ZnO@AC was used. With SnO_2@AC, other acetals were also detected from the reaction solution (see GC-MS Fig. S7). The formation of Brønsted acid, i.e. formation of HCl from $SnCl_2$ on the surface of SnO_2@AC and H_2O produced as a by-product in the formation of ethyl lactate might catalyze the dehydration reaction to form HMF and ethyl levulinate [23]. These types of side reactions from fructose and glucose

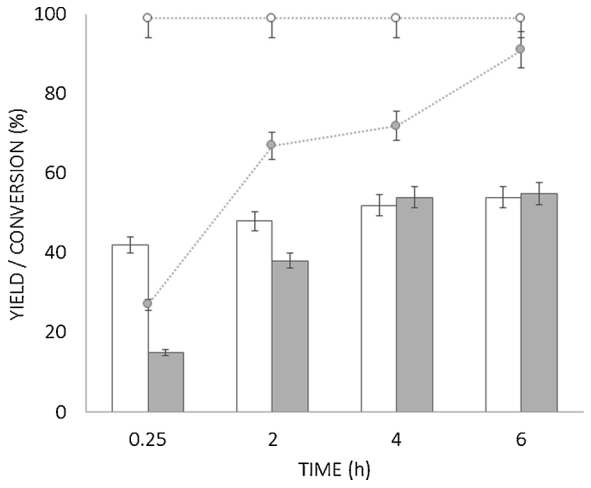

Fig. 2. The yield (bars) and conversion (dots) of fructose to ethyl lactate with SnO_2@AC (white bars and dots) and ZnO@AC (gray bars and dots) catalysts. (0.55 mmol fructose; 0.1 g catalyst; 20 mL EtOH; 160 °C; N_2).

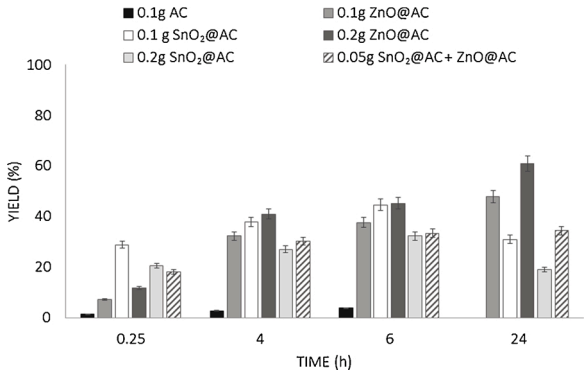

Fig. 3. Yield of ethyl lactate from glucose conversion by using AC and SnO_2@AC and ZnO@AC catalyst (0.55 mmol glucose; 0.1 g, 0.2 g or combination of 0.05 g of catalysts; 20 mL EtOH; 160 °C; N_2).

are usually said to lead to the formation of humins and subsequent catalyst deactivation [47]. However, only a small amount of Cl^- was leached to the reaction mixture (< 10 ppm), indicating that the formation of HCl as Brønsted acid was not notable. This was suggesting that HNO_3 modified carbon support together with acidic $SnCl_2$ impregnation solution in the preparation step were able to create new more acidic surface groups to the catalyst as seen from the characterization results (e.g. NH_3-TPD). These acidic groups could direct the reaction toward furan derivative formation as discussed in the literature that dehydration reactions towards HMF are favored by Sn-catalysts with Brønsted acidity [48].

The reaction studies with glucose conversion continued with the ZnO@AC catalyst. High conversion of glucose was obtained when a higher amount of catalyst (0.2 g) was added to the reaction (Fig. 3). The yield of ethyl lactate increased to 46% in 6 h, which was the same as that obtained with the SnO_2@AC catalyst in 6 h. When the reaction was continued to 24 h, the yield was increased to 61%. This was a significantly higher yield obtained from glucose conversion when compared, for example, to the yield obtained with beta-zeolites. With Sn-Beta-H, an ethyl lactate yield of 29% was obtained from glucose conversion at 160 °C N_2 in 10 h [19]. Further, with Sn-Beta, 37% ethyl lactate yield was obtained from glucose at 160 °C, 10 bar N_2, in 20 h [20]. Notably, the highest yield obtained from glucose found in the literature was 41% with Sn-Beta-H (5 bar N_2, 160 °C, 10 h) [21]. Thus, our activated carbon-based catalysts provided high yields of ethyl lactate.

With the SnO_2@AC catalyst, the yield decreased from 45% to 32% when a higher amount of catalyst (from 0.1 g to 0.2 g) was added into the glucose conversion reaction. After 24 h, the yield was even lower, 19% (Fig.3). This indicated that the reaction was going in another direction, producing more furan derivatives.

In the studies by Prudius et al. [22], higher yields were obtained by combining the two metal oxides—SnO_2 and ZnO—in the same catalyst, and the yield of ethyl lactate from fructose increased from 32% to 56%, respectively, compared to a single metal Sn oxide catalyst. The effect of the combination of Sn and Zn oxides on the conversion and selectivity to ethyl lactate was studied by using a mixture of 0.05 g SnO_2@AC and 0.05 g ZnO@AC (Fig. 3). In our experiment, no such increase with combination tin and zinc oxide catalysts was detected; in fact, the yield was now 31% and was lower than by single metal oxide catalysts in ethyl lactate production from glucose. The addition of Zn to Sn-Beta zeolite has been shown to enhance the strength of base sites besides Lewis acid sites, which may inhibit the formation of other products, such as HMF and its subsequent decomposition [49]. It is possible that in our ZnO@AC catalyst, the milder acidity together with mild basicity was favorable for the ethyl lactate production from hexoses preventing byproducts such as furan derivatives compared to the SnO_2@AC with higher acidity, which, by contrast, directed the reaction toward the furan derivative formation.

In our previous study [27] of glucose conversion in aqueous solution, the activated carbon-based metal oxide catalyst containing Sn or Zn oxides 5–10 wt.% was used, and the obtained lactic acid yields were less than 30%. The highest yield of lactic acid from glucose in aqueous solution was obtained using the dual metal catalyst containing Sn and Al oxides on AC, and was 42%. However, the catalyst was not stable in recycle experiments. In this study, the glucose conversion in EtOH with single metal oxides Sn and Zn on AC, the maximum yield of ethyl lactate obtained, was 45% with SnO_2@AC and 61% with the ZnO@AC. That is, the yields were much higher in EtOH than in aqueous phase. Previous studies have suggested that the esterification reaction producing alkyl lactates is more quantitative than the dehydration–hydration route, which produces lactic acid [50].

Reusability tests of the SnO_2@AC and ZnO@AC catalysts were performed to obtain information about the stability of the catalyst. The recycling experiments were conducted using the amount of the catalyst that produced the best yield of ethyl lactate in the glucose conversion, which was 0.1 g for SnO_2@AC and 0.2 g for ZnO@AC (Fig.4).

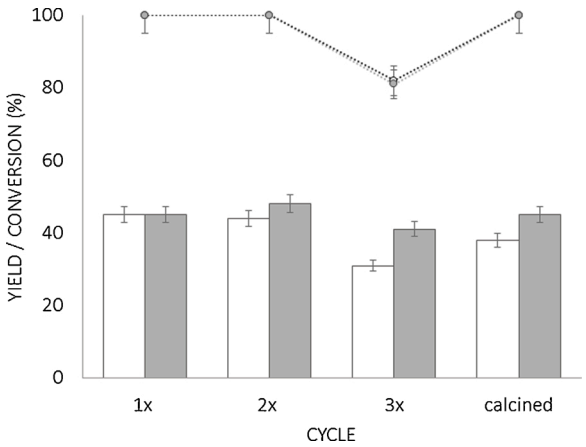

Fig. 4. The conversion (dots) and yield (bars) of ethyl lactate in recycling experiments of catalysts SnO_2@AC (white) and ZnO@AC (gray) from glucose (0.1 g) in 20 mL EtOH at 160 °C, N_2, 600 rpm, and 6 h.

Experiments were performed in EtOH at 160 °C, N_2, 600 rpm for 6 h. The catalyst was recycled in the reaction three times, using the same conditions in every cycle. The ZnO@AC maintained the selectivity to ethyl lactate; however, with the SnO_2@AC, a slight decrease in the yield was obtained during the recycling. The conversion decreased slightly with both catalysts, from 100% to 82%. After the third cycle, the catalysts were calcined under air at 300 °C for 2 h, and the conversion and yield increased back to the initial level; however, with tin catalyst, a slightly lower yield was obtained even after calcination. ZnO@AC obtained slightly better recyclability in recycling experiments than SnO_2@AC, and this could be because of the higher production of the byproducts in the process with tin catalyst, which could end up to humin formation and subsequently deactivating the catalyst [27]. The stability of the active sites on activated carbon support was studied after catalyst use. The reaction liquid was analyzed using the ICP-OES method and the metal content was determined. After the run, 0.9 % of both tin and aluminum was leached from the initial metal content added to the catalysts. This was indicating that no significant loss of metal occurred during the use. Overall, no major decrease was observed in the recycling experiments.

3.2.3. *Hydrolysate conversion*

Real biomass hydrolysates of the fiber sludge and spruce were tested in the conversion to ethyl lactate with Sn and Zn oxide catalysts. The contents of the hydrolysates are presented in Table S2 in Supplementary material. Fiber sludge hydrolysate mainly contained glucose and a small amount of lactic acid. Glucose was also the main component of the spruce hydrolysate with a small amount hemicellulose sugars—arabinose, galactose, and sucrose—detected from the hydrolysate (~2 wt.% combined). Lactic acid, HMF, and levulinic acid were also present in spruce hydrolysate in small amounts (approx. 1–2 wt.% of each). The pH of the hydrolysate solutions was 3.2 for fiber sludge and 4.9 for spruce. The inorganic content of the hydrolytes was analyzed by ICP analysis and ion chromatography analysis. The results revealed that both hydrolysates contained Na^+ cations and SO_4^{2-} anions (Table S2), and a higher contents of these ions were detected in fiber sludge hydrolysate than in spruce (0.25 and 0.08 wt.% Na^+ and 0.52 and 0.25 wt. % SO_4^{2-}, respectively). These were the residual contents from the preparation processes of the hydrolysates.

The conversion reactions were performed by using 0.1 g of SnO_2@AC or 0.2 g ZnO@AC of the catalyst in the reactor at 160 °C, N_2 and hydrolysate was added to 20 mL EtOH containing similar amounts of glucose as in the model solution experiments with hexoses (0.55 mmol). The samples from the reaction mixture were taken after 15 min, 6 h, and 24 h, and the liquid product mixture was analyzed with HPLC and GC-

MS. The results of the experiments and quantified product yields with HPLC are presented in Fig. 5. The reaction mixture from the fiber sludge hydrolysate converted with ZnO@AC contained mainly ethyl lactate as a product, and the yield was 84% after 24 h (Fig. 5a). Ethyl lactate was the main product also in the spruce hydrolysate conversion after 24 h and the yield was 86% (Fig. 5b). When the samples of the product mixtures were analyzed with GC-MS and compared to model solutions from hexoses, the absence of acetal in the reaction mixture was observed in all experiments, and the main product was ethyl lactate for both hydrolysates (Fig. S8 Supplementary material). With the SnO_2@AC catalyst, the reaction mixture from hydrolysate conversion after 6 h or 24 h contained less ethyl lactate compared to ZnO@AC catalyst. After 6 h, the yield from the fiber sludge conversion was only 29% and did not increase remarkably when the reaction was continued to 24 h (Fig. 5c). Similarly, from the conversion of spruce hydrolysate, the yield with SnO_2@AC was only 17% after 6 h and 24% after 24 h (Fig.5 d). These yields were much lower than those obtained from the model solution conversion reactions with SnO_2@AC. Further, in this case, the byproduct formation of furfural, HMF, and ethyl levulinate was detected and was more prominent compared to ZnO@AC. However, the formation of acetal was not detected when using the hydrolysates with SnO_2@AC, similarly as with ZnO@AC (see GC-MS Fig. S9).

The reason for such high yields of alkyl lactate and suppressed acetal formation has been suggested to result from the alkali medium, which promotes the isomerization of hemiacetal to ethyl lactate instead of acetal formation [51]; however, in our studies, the reaction media was on the acidic side. In other studies, it has been noted that the presence of alkali salts in the reaction had a significant effect on the selectivity to alkyl lactate or lactic acid formation [22,24]. It was proposed that possibly the neutralization of Brønsted acidity from the catalyst framework by cations and/or increased Brønsted basicity (SO_4^{2-}) in the reaction solution resulted in this significant increase as well as inhibition of hexose dehydration to side products [24,52]. Similar increase in ethyl lactate yield was noticed in our experiments when using hydrolysates of spruce and fiber sludge. However, this trend was noticed only with ZnO@AC but not with SnO_2@AC. In fact, the yield was lower for the SnO_2@AC catalyst when compared to the yield from the model solutions. Analysis of the used hydrolysates revealed residual Na^+ and SO_4^{2-} ion contents from the preparation/pretreatment process. The impact of the addition of Na_2SO_4 salt in the reaction was tested in glucose conversion by adding similar amounts of ions Na^+ and SO_4^{2-} as in the fiber sludge hydrolysate (0.05 mmol Na_2SO_4 and 0.55 mmol glucose in 20 mL of EtOH at 160 °C N_2 and 0.1 g of SnO_2@AC or 0.2 g of ZnO@AC). As a result, an increased ethyl lactate yield of 78% was observed from the reaction mixture of ZnO@AC, as observed with the hydrolysates. With the SnO_2@AC catalyst, the addition of Na_2SO_4 decreased the ethyl lactate yield, as was noted with the hydrolysates. The salts added to the reaction have been noted to increase lactate yield, although Tolborg et al. noted that the amount of salt needed to be optimized for every salt and each specific catalyst [24]. This may explain why the addition of salt with SnO_2@AC catalyst did not have a similar positive effect to the lactate yield as was detected with ZnO@AC. To examine this phenomenon, a higher amount of Na_2SO_4 (0.2 mmol vs. 0.05 mmol) was added to the glucose conversion reaction (0.55 mmol glucose in 20 mL of EtOH at 160 °C and 0.1 g of catalyst). Results of the hydrolysate conversions are presented in Fig. 6. This time, the SnO_2@AC catalyst was able to convert glucose to ethyl lactate with a 54% yield and ZnO@AC with 51% (note that the lower amount of catalyst ZnO@AC was used in this experiment: 0.1 g vs. 0.2 g) (Fig. 6). This indicates that the amount of salt needs to be optimized for each catalysts. The exact mechanism of salt's improvement toward selectivity of ethyl lactate together with

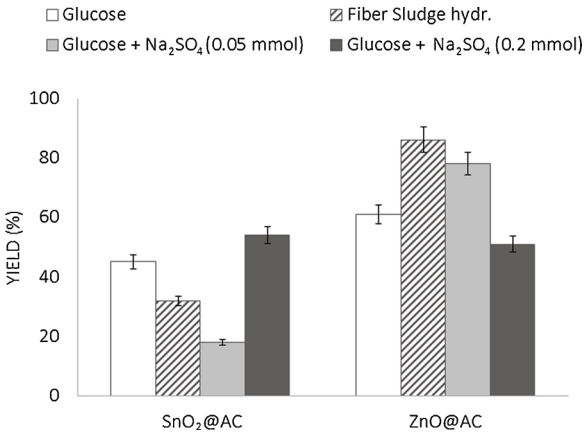

Fig. 6. Effect of the Na_2SO_4 to yield of ethyl lactate in the reaction with SnO_2@AC and ZnO@AC catalysts (0.55 mmol glucose; 0.05 or 0.2 mmol Na_2SO_4; 20 mL EtOH; N_2; 160 °C and 0.1 g SnO_2@AC or 0.2 g ZnO@AC (with 0.2 mmol Na_2SO_4 0.1 g of ZnO@AC was used)).

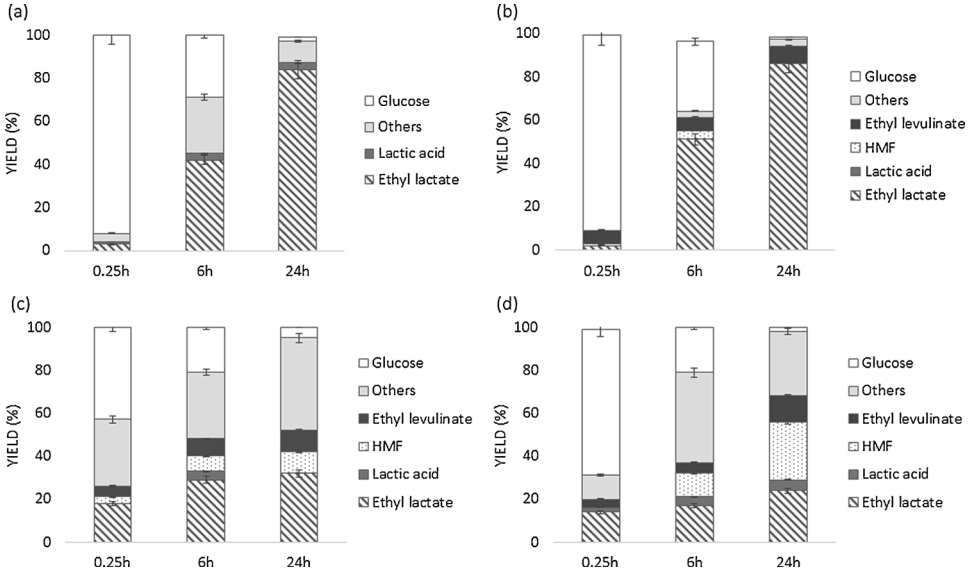

Fig. 5. Conversion of fiber sludge (a) and spruce hydrolysate (b) with ZnO@AC catalyst and conversion of fiber sludge (c) and spruce hydrolysate (d) with SnO_2@AC catalyst (0.55 mmol glucose in hydrolysate, EtOH, 0.1 g SnO_2@AC or 0.2 g ZnO@AC; N_2; 160 °C).

catalysts is still not clear and future research is needed on the topic. Further, it must be taken into account that the salt Na_2SO_4 in the solution is not possibly the only factor affecting the ethyl lactate yield since the hydrolysates also contained other compounds (other anions and cations and organic molecules) in lesser amounts.

Overall, these findings show that the catalysts could be used directly in the conversion of real biomass hydrolysates from the process when optimized.

The proposed reaction scheme for the conversion of lignocellulosic biomass-based hexoses and trioses to ethyl lactate and the main byproducts in the reaction are presented in Scheme 2. With a highly acidic catalyst, the reaction produced furan derivatives such as ethyl levulinate as a byproduct. In acidic conditions, acetals were produced as byproduct. The suggested reaction route and the reaction products were rather similar to those suggested by Younas et al.[23]. However, in this study, it was noted that in the presence of salt Na_2SO_4 (Na^+ cations and weakly basic anions, SO_4^{2-}) in the reaction solution, the unwanted acetal production was suppressed and the ethyl lactate production increased. The main reaction from glucose to ethyl lactate is mainly catalyzed by Lewis acid sites, which also catalyze the retro aldol condensation.

Lastly, recycling experiments of the ZnO@AC catalyst in the conversion of fiber sludge hydrolysate were selected to perform, since fewer byproducts were formed when using fiber sludge hydrolysate. We observed that the catalyst retained its properties in three recycling experiments without the notable loss of activity, biomass conversion, or ethyl lactate selectivity at the studied conditions (Fig. 7). To investigate the catalyst stability, the amount of metal that had leached into the reaction liquid was determined by ICP-OES. After the first run, a small amount of zinc metal, approximately 2% of the initial amount added to the catalyst, was detected from the solution and was approximately the same after the second and third run. Further, more studies are needed to investigate the long-term stability of the catalysts. In addition, studies with substrates that are more concentrated is needed to fully understand the potential of these catalysts.

4. Conclusions

The aim of this study was to produce heterogeneous carbon-based catalysts for the production of ethyl lactate from lignocellulosic precursors. As catalysts, biomass-based carbon-supported Sn and Zn oxide catalysts were prepared from hydrolysis lignin and tested for conversion of model solutions of trioses and hexoses and real biomass hydrolysates of lignocellulosic biomass to ethyl lactate. Both SnO_2@AC and ZnO@AC

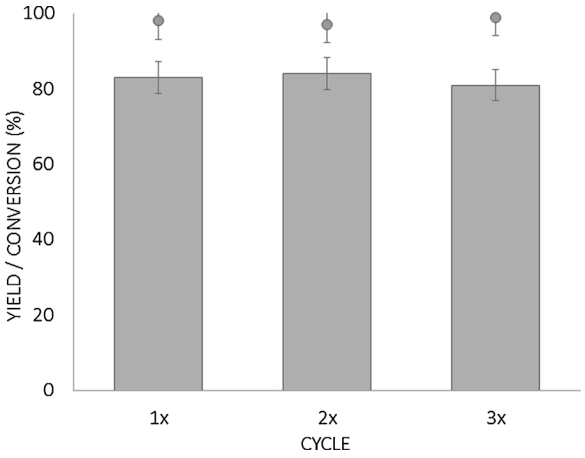

Fig. 7. Conversion (dots) and yield (bars) of the recycling experiment with ZnO@AC catalyst in three cycles in fiber sludge hydrolysate (0.55 mmol glucose in hydrolysate, 20 mL EtOH, 0.2 g cat.; N_2; 160 °C).

were able to produce ethyl lactate in good yields; however, the activity and selectivity for precursor substrate differed in each. SnO_2@AC was more active and selective in triose (dihydroxyacetone) conversion and provided 99% yield and selectivity to ethyl lactate. ZnO@AC, by contrast, was more selective than SnO_2@AC in glucose conversion, providing a 60% yield of ethyl lactate. The stronger acidity of the SnO_2@AC guided the production of furan derivatives, such as HMF and ethyl levulinate from hexoses. In acidic conditions, acetal production was also present as a byproduct for both catalysts. When lignocellulose-derived solutions (spruce or fiber sludge hydrolysate) were tested, the yields of ethyl lactate were significantly higher (approximately 85%) when using ZnO@AC catalyst than those from the optimized model solution experiments. These hydrolysate solutions contained residual levels of Na^+ and SO_4^{2-} ions from the preparation process of hydrolysates, which was most likely the cause of the higher yield of ethyl lactate in the process. The salt originated from biomass-derived hydrolysates suppressed the acetal formation and resulted in higher ethyl lactate selectivity. Finally, the reusability of the catalyst was studied in hexose and hydrolysate conversion, with the catalysts successfully maintaining their catalytic activity at studied conditions.

These findings open the door to future studies with activated carbon-supported catalysts to obtain high ethyl lactate yields. Furthermore, we

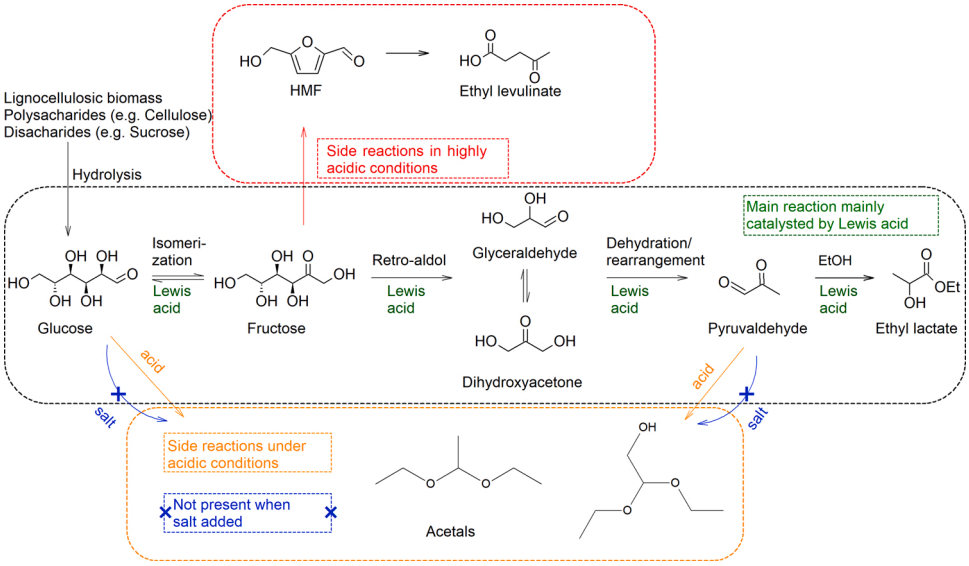

Scheme 2. The proposed reaction route from biomass-based molecules and the main byproducts in the reaction [23].

demonstrated that heterogeneous activated carbon metal oxide catalysts could be applied to the catalytic conversion reaction of biomass hydrolysates to ethyl lactate with high yields for biorefinery applications.

CRediT authorship contribution statement

Riikka Kupila: Conceptualization, Investigation, Formal analysis, Data curation, Visualization, Writing - original draft, Writing - review & editing. **Katja Lappalainen:** Conceptualization, Supervision, Writing - review & editing. **Tao Hu:** Formal analysis, Writing - review & editing. **Anne Heponiemi:** Formal analysis, Writing - review & editing. **Davide Bergna:** Formal analysis, Writing - review & editing. **Ulla Lassi:** Supervision, Writing - review & editing.

Declaration of Competing Interest

The authors report no declarations of interest.

Acknowledgements

Authors R.K. and K.L. would like to thank the Green Bioraff Solutions Project (EU/Interreg/Botnia-Atlantica, 20201508) for funding this research. Ilkka Vesavaara is thanked for ICP-OES analysis. Centria University of Applied Sciences is thanked for equipment use, and Leif Hed and Ritva Mäkelä with the help of analytics with GC-MS and electrophoresis analysis. Sari Tuikkanen is thanked for performing the ion chromatography analysis.

Appendix A. Supplementary data

Supplementary material related to this article can be found, in the online version, at doi:https://doi.org/10.1016/j.apcata.2021.118327.

References

[1] C.S.M. Pereira, V.M.T.M. Silva, A.E. Rodrigues, Ethyl lactate as a solvent: Properties, applications and production processes – a review, Green Chem. 13 (2011) 2658–2671, https://doi.org/10.1039/C1GC15523G.
[2] M.S. Holm, Y.J. Pagán-Torres, S. Saravanamurugan, A. Riisager, J.A. Dumesic, E. Taarning, Sn-Beta catalysed conversion of hemicellulosic sugars, Green Chem. 14 (2012) 702–706, https://doi.org/10.1039/C2GC16202D.
[3] L. Li, C. Stroobants, K. Lin, P.A. Jacobs, B.F. Sels, P.P. Pescarmona, Selective conversion of trioses to lactates over Lewis acid heterogeneous catalysts, Green Chem. 13 (2011) 1175–1181, https://doi.org/10.1039/C0GC00923G.
[4] S. Li, W. Deng, Y. Li, Q. Zhang, Y. Wang, Catalytic conversion of cellulose-based biomass and glycerol to lactic acid, J. Energy Chem. 32 (2019) 138–151, https://doi.org/10.1016/J.JECHEM.2018.07.012.
[5] J.J. Bozell, G.R. Petersen, Technology development for the production of biobased products from biorefinery carbohydrates—the US Department of Energy's "Top 10" revisited, Green Chem. 12 (2010) 539–554, https://doi.org/10.1039/B922014C.
[6] A.V. Dolzhenko, Ethyl lactate and its aqueous solutions as sustainable media for organic synthesis, Sustain. Chem. Pharm. 18 (2020), 100322, https://doi.org/10.1016/j.scp.2020.100322.
[7] C.S.M. Pereira, A.E. Rodrigues, Ethyl Lactate Main Properties, Production Processes, and Applications, in: F. Chemat, M.A. Vian (Eds.), Altern. Solvents Nat. Prod. Extr., Alternativ, Springer Berlin Heidelberg, Berlin, Heidelberg, 2014, pp. 107–125, https://doi.org/10.1007/978-3-662-43628-8.
[8] S. Aparicio, Computational Study on the Properties and Structure of Methyl Lactate, J. Phys, Chem. A. 111 (2007) 4671–4683, https://doi.org/10.1021/jp070841t.
[9] A. Corma Canos, S. Iborra, A. Velty, Chemical routes for the transformation of biomass into chemicals, Chem. Rev. 107 (2007) 2411–2502, https://doi.org/10.1021/cr050989d.
[10] J.H. Clark, S.J. Tavener, Alternative Solvents: Shades of Green, Org. Process Res. Dev. 11 (2007) 149–155, https://doi.org/10.1021/op060160g.
[11] M. Dusselier, P. Van Wouwe, A. Dewaele, E. Makshina, B.F. Sels, Lactic acid as a platform chemical in the biobased economy: the role of chemocatalysis, Energy Environ. Sci. 6 (2013) 1415–1442, https://doi.org/10.1039/C3EE00069A.
[12] K.L. Wasewar, A.A. Yawalkar, J.A. Moulijn, V.G. Pangarkar, Fermentation of Glucose to Lactic Acid Coupled with Reactive Extraction: A Review, Ind. Eng. Chem. Res. 43 (2004) 5969–5982, https://doi.org/10.1021/ie049963n.
[13] P. Mäki-Arvela, I.L. Simakova, T. Salmi, D.Y. Murzin, Production of Lactic Acid/Lactates from Biomass and Their Catalytic Transformations to Commodities, Chem. Rev. 114 (2014) 1909–1971, https://doi.org/10.1021/cr400203v.
[14] M.S. Holm, S. Saravanamurugan, E. Taarning, Conversion of Sugars to Lactic Acid Derivatives Using Heterogeneous Zeotype Catalysts, Science (80-.) 328 (2010) 602–605, https://doi.org/10.1126/science.1183990.
[15] K. Nemoto, Y. Hirano, K. Hirata, T. Takahashi, H. Tsuneki, K. Tominaga, K. Sato, Cooperative In–Sn catalyst system for efficient methyl lactate synthesis from biomass-derived sugars, Appl. Catal. B Environ. 183 (2016) 8–17, https://doi.org/10.1016/J.APCATB.2015.10.015.
[16] P. Mäki-Arvela, A. Aho, D.Y. Murzin, Heterogeneous Catalytic Synthesis of Methyl Lactate and Lactic Acid from Sugars and Their Derivatives, ChemSusChem. 13 (2020) 4833–4855, https://doi.org/10.1002/cssc.202001223.
[17] F. de Clippel, M. Dusselier, R. Van Rompaey, P. Vanelderen, J. Dijkmans, E. Makshina, L. Giebeler, S. Oswald, G.V. Baron, J.F.M. Denayer, P.P. Pescarmona, P.A. Jacobs, B.F. Sels, Fast and Selective Sugar Conversion to Alkyl Lactate and Lactic Acid with Bifunctional Carbon–Silica Catalysts, J. Am, Chem. Soc. 134 (2012) 10089–10101, https://doi.org/10.1021/ja301678w.
[18] E. Pighin, V.K. Díez, J.I. Di Cosimo, Kinetic study of the ethyl lactate synthesis from triose sugars on Sn/Al2O3 catalysts, Catal. Today. 289 (2017) 29–37, https://doi.org/10.1016/J.CATTOD.2016.10.002.
[19] X. Yang, Y. Liu, X. Li, J. Ren, L. Zhou, T. Lu, Y. Su, Synthesis of Sn-Containing Nanosized Beta Zeolite As Efficient Catalyst for Transformation of Glucose to Methyl Lactate, ACS Sustain. Chem. Eng. 6 (2018) 8256–8265, https://doi.org/10.1021/acssuschemeng.8b00177.
[20] J. Zhang, L. Wang, G. Wang, F. Chen, J. Zhu, C. Wang, C. Bian, S. Pan, F.-S. Xiao, Hierarchical Sn-Beta Zeolite Catalyst for the Conversion of Sugars to Alkyl Lactates, ACS Sustain, Chem. Eng. 5 (2017) 3123–3131, https://doi.org/10.1021/acssuschemeng.6b02881.
[21] X. Yang, J. Bian, J. Huang, W. Xin, T. Lu, C. Chen, Y. Su, L. Zhou, F. Wang, J. Xu, Fluoride-free and low concentration template synthesis of hierarchical Sn-Beta zeolites: efficient catalysts for conversion of glucose to alkyl lactate, Green Chem. 19 (2017) 692–701, https://doi.org/10.1039/C6GC02437H.
[22] V.S. Prudius, L.N. Hes, V.V. Brei, Conversion of D-Fructose into Ethyl Lactate Over a Supported SnO2–ZnO/Al2O3 Catalyst, Colloids and Interfaces 3 (2019), https://doi.org/10.3390/colloids3010016.
[23] R. Younas, L. Huang, K. Zhang, L. Cao, L. Zhang, M. Khan, H. Xu, S. Zhang, Selective Production of Ethyl Lactate from Rice Straw in the Presence of Lewis and Brønsted Acids, Waste and Biomass Valorization (2019), https://doi.org/10.1007/s12649-019-00898-1.
[24] S. Tolborg, I. Sádaba, C.M. Osmundsen, P. Fristrup, M.S. Holm, E. Taarning, Tin-containing Silicates: Alkali Salts Improve Methyl Lactate Yield from Sugars, ChemSusChem. 8 (2015) 613–617, https://doi.org/10.1002/cssc.201403057.
[25] P. Sudarsanam, R. Zhong, S. Van Den Bosch, S.M. Coman, V.I. Parvulescu, B.F. Sels, Functionalised heterogeneous catalysts for sustainable biomass valorisation, Chem. Soc. Rev. 47 (2018) 8349, https://doi.org/10.1039/c8cs00410b.
[26] Z. Wang, G. Wu, L.J. Jönsson, Effects of impregnation of softwood with sulfuric acid and sulfur dioxide on chemical and physical characteristics, enzymatic digestibility, and fermentability, Bioresour. Technol. 247 (2018) 200–208, https://doi.org/10.1016/j.biortech.2017.09.081.
[27] R. Kupila, K. Lappalainen, T. Hu, H. Romar, U. Lassi, Lignin-based activated carbon-supported metal oxide catalysts in lactic acid production from glucose, Appl. Catal. A Gen. 612 (2021), 118011, https://doi.org/10.1016/j.apcata.2021.118011.
[28] H.T. Gomes, S.M. Miranda, M.J. Sampaio, A.M.T. Silva, J.L. Faria, Activated carbons treated with sulphuric acid: Catalysts for catalytic wet peroxide oxidation, Catal. Today. 151 (2010) 153–158, https://doi.org/10.1016/j.cattod.2010.01.017.
[29] A.M. Oickle, S.L. Goertzen, K.R. Hopper, Y.O. Abdalla, H.A. Andreas, Standardization of the Boehm titration: Part II. Method of agitation, effect of filtering and dilute titrant, Carbon N. Y. 48 (2010) 3313–3322, https://doi.org/10.1016/j.carbon.2010.05.004.
[30] J. Schönherr, J. Buchheim, P. Scholz, P. Adelhelm, Boehm Titration Revisited (Part II): A Comparison of Boehm Titration with Other Analytical Techniques on the Quantification of Oxygen-Containing Surface Groups for a Variety of Carbon Materials, C. 4, 2018, p. 22, https://doi.org/10.3390/c4020022.
[31] U. Zielke, K.J. Hüttinger, W.P. Hoffman, Surface-oxidized carbon fibers: I. Surface structure and chemistry, Carbon N. Y. 34 (1996) 983–998, https://doi.org/10.1016/0008-6223(96)00032-2.
[32] R. Tian, Y. Zhang, Z. Chen, H. Duan, B. Xu, Y. Guo, H. Kang, H. Li, H. Liu, The effect of annealing on a 3D SnO2/graphene foam as an advanced lithium-ion battery anode, Sci. Rep. 6 (2016), 19195, https://doi.org/10.1038/srep19195.
[33] J. Guo, P. Li, L. Chai, Y. Su, J. Diao, X. Guo, Silica template-assisted synthesis of SnO2@porous carbon composites as anode materials with excellent rate capability and cycling stability for lithium-ion batteries, RSC Adv. 7 (2017) 30070–30079, https://doi.org/10.1039/C7RA03594B.
[34] R. Al-Gaashani, S. Radiman, A.R. Daud, N. Tabet, Y. Al-Douri, XPS and optical studies of different morphologies of ZnO nanostructures prepared by microwave methods, Ceram. Int. 39 (2013) 2283–2292, https://doi.org/10.1016/j.ceramint.2012.08.075.
[35] L. Chen, Z. Yang, L. Wang, H. Qin, Rational synthesis of 3D ZnO-Cu-C yolk-shell hybrid microspheres and their high performance as anode material for zinc-nickel secondary batteries, Ceram. Int. 45 (2019) 10792–10799, https://doi.org/10.1016/j.ceramint.2019.02.153.
[36] M.A. Montes-Morán, D. Suárez, J. Angel Menéndez, E. Fuente, Chapter 6, in: J.M.D. B.T.-N.C.A. Tascón (Ed.), The Basicity of Carbons, Elsevier, Oxford, 2012, pp. 173–203, https://doi.org/10.1016/B978-0-08-097744-7.00006-5.
[37] E. Taarning, S. Saravanamurugan, M. Spangsberg Holm, J. Xiong, R.M. West, C. H. Christensen, Zeolite-Catalyzed Isomerization of Triose Sugars, ChemSusChem. 2 (2009) 625–627, https://doi.org/10.1002/cssc.200900099.

[38] A. Feliczak-Guzik, M. Sprynskyy, I. Nowak, B. Buszewski, Catalytic Isomerization of Dihydroxyacetone to Lactic Acid and Alkyl Lactates over Hierarchical Zeolites Containing Tin, Catal. 8 (2018), https://doi.org/10.3390/catal8010031.
[39] V.M.T.M. Silva, A.E. Rodrigues, Synthesis of diethylacetal: thermodynamic and kinetic studies, Chem. Eng. Sci. 56 (2001) 1255–1263, https://doi.org/10.1016/S0009-2509(00)00347-X.
[40] M.R. Capeletti, L. Balzano, G. de la Puente, M. Laborde, U. Sedran, Synthesis of acetal (1,1-diethoxyethane) from ethanol and acetaldehyde over acidic catalysts, Appl. Catal. A Gen. 198 (2000) L1–L4, https://doi.org/10.1016/S0926-860X(99)00502-5.
[41] J. Ob-eye, P. Praserthdam, B. Jongsomjit, Dehydrogenation of Ethanol to Acetaldehyde over Different Metals Supported on Carbon Catalysts, Catal. 9 (2019), https://doi.org/10.3390/catal9010066.
[42] T. Riittonen, E. Toukoniitty, D.K. Madnani, A.-R. Leino, K. Kordas, M. Szabo, A. Sapi, K. Arve, J. Wärnå, J.-P. Mikkola, One-Pot Liquid-Phase Catalytic Conversion of Ethanol to 1-Butanol over Aluminium Oxide—The Effect of the Active Metal on the Selectivity, Catal. 2 (2012), https://doi.org/10.3390/catal2010068.
[43] F. Carrasco-Marín, A. Mueden, C. Moreno-Castilla, Surface-Treated Activated Carbons as Catalysts for the Dehydration and Dehydrogenation Reactions of Ethanol, J. Phys. Chem. B. 102 (1998) 9239–9244, https://doi.org/10.1021/jp9818611.
[44] X. Cao, X. Peng, S. Sun, L. Zhong, W. Chen, S. Wang, R.-C. Sun, Hydrothermal conversion of xylose, glucose, and cellulose under the catalysis of transition metal sulfates, Carbohydr. Polym. 118 (2015) 44–51, https://doi.org/10.1016/j.carbpol.2014.10.069.
[45] Z. Srokol, A.-G. Bouche, A. van Estrik, R.C.J. Strik, T. Maschmeyer, J.A. Peters, Hydrothermal upgrading of biomass to biofuel; studies on some monosaccharide model compounds, Carbohydr. Res. 339 (2004) 1717–1726, https://doi.org/10.1016/j.carres.2004.04.018.
[46] M. Dusselier, P. Van Wouwe, A. Dewaele, E. Makshina, B.F. Sels, Lactic acid as a platform chemical in the biobased economy: The role of chemocatalysis, Energy Environ. Sci. 6 (2013) 1415–1442, https://doi.org/10.1039/c3ee00069a.
[47] F. Shahangi, A. Najafi Chermahini, M. Saraji, Dehydration of fructose and glucose to 5-hydroxymethylfurfural over Al-KCC-1 silica, J. Energy Chem. 27 (2018) 769–780, https://doi.org/10.1016/j.jechem.2017.06.004.
[48] A.A. Marianou, C.M. Michailof, A. Pineda, E.F. Iliopoulou, K.S. Triantafyllidis, A. A. Lappas, Effect of Lewis and Brønsted acidity on glucose conversion to 5-HMF and lactic acid in aqueous and organic media, Appl. Catal. A Gen. 555 (2018) 75–87, https://doi.org/10.1016/J.APCATA.2018.01.029.
[49] W. Dong, Z. Shen, B. Peng, M. Gu, X. Zhou, B. Xiang, Y. Zhang, Selective Chemical Conversion of Sugars in Aqueous Solutions without Alkali to Lactic Acid Over a Zn-Sn-Beta Lewis Acid-Base Catalyst, Sci. Rep. 6 (2016) 26713, https://doi.org/10.1038/srep26713.
[50] R.M. West, M.S. Holm, S. Saravanamurugan, J. Xiong, Z. Beversdorf, E. Taarning, C.H. Christensen, Zeolite H-USY for the production of lactic acid and methyl lactate from C3-sugars, J. Catal. 269 (2010) 122–130, https://doi.org/10.1016/J.JCAT.2009.10.023.
[51] A.M. Mylin, S.I. Levytska, M.E. Sharanda, V.V. Brei, Selective conversion of dihydroxyacetone–ethanol mixture into ethyl lactate over amphoteric ZrO2–TiO2 catalyst, Catal. Commun. 47 (2014) 36–39, https://doi.org/10.1016/j.catcom.2014.01.004.
[52] A. Kohler, W. Seames, I. Foerster, C. Kadrmas, Catalytic Formation of Lactic and Levulinic Acids from Biomass Derived Monosaccarides through Sn-Beta Formed by Impregnation, Catal. 10 (2020), https://doi.org/10.3390/catal10101219.